

# **Load Feedback from a Dynamically Scaled Robotic Model of** *Carausius Morosus* **Middle Leg**

William P. Zyhowski<sup>1(⊠)</sup>, Sasha N. Zill<sup>2</sup>, and Nicholas S. Szczecinski<sup>1</sup>

 West Virginia University, Morgantown, WV 26506, USA wz00007@mix.wvu.edu
Marshall University, Huntington, WV 25755, USA

Abstract. Load sensing is critical for walking behavior in animals, who have evolved a number of sensory organs and neural systems to improve their agility. In particular, insects measure load on their legs using campaniform sensilla (CS), sensory neurons in the cuticle of high-stress portions of the leg. Extracellular recordings from these sensors in a behaving animal are difficult to collect due to interference from muscle potentials, and some CS groups are largely inaccessible due to their placement on the leg. To better understand what loads the insect leg experiences and what sensory feedback the nervous system may receive during walking, we constructed a dynamically-scaled robotic model of the leg of the stick insect Carausius morosus. We affixed strain gauges in the same positions and orientations as the major CS groups on the leg, i.e., 3, 4, 6A, and 6B. The robotic leg was mounted to a vertically-sliding linear guide and stepped on a treadmill to simulate walking. Data from the strain gauges was run through a dynamic model of CS discharge developed in a previous study. Our experiments reveal stereotypical loading patterns experienced by the leg, even as its weight and joint stiffness is altered. Furthermore, our simulated CS strongly signal the beginning and end of stance phase, two key events in the coordination of walking.

**Keywords:** Campaniform sensilla  $\cdot$  Insects  $\cdot$  Dynamic scaling  $\cdot$  Strain gauges  $\cdot$  Legged locomotion  $\cdot$  Robotics

#### 1 Introduction

Locomotion is fundamentally an interaction with the environment, which is a challenge for animals and robots alike. Animals have evolved a wide array of sensory organs and neural control systems that give them an innate ability to solve this problem [1–3]. Robots, on the other hand, need to be meticulously designed to accomplish these feats. By constructing robotic models of animals, it may be possible to better understand how their sensors and nervous systems function and simultaneously build robots that leverage biological mechanisms to maneuver more capably.

Load sensing is critical for walking animals [1, 4]. Insects measure this load using campaniform sensilla (CS). CS are not simple sensors; in fact, they measure force in a highly dynamic way [5]. Due to their dynamics, CS are very sensitive to changes in force,

© The Author(s), under exclusive license to Springer Nature Switzerland AG 2022 A. Hunt et al. (Eds.): Living Machines 2022, LNAI 13548, pp. 128–139, 2022. https://doi.org/10.1007/978-3-031-20470-8 14 including transient changes in the effect of body weight [6], movements of the substrate under their feet [7], and small variations in bending moments on each leg segment that naturally occur over the course of a step [5]. In a previous study, we made a CS model of how the forces on the leg are transduced into neural signals [8]. Related CS models describe how forces on the halteres of dipterans are transduced into signals [3]. Such models give insight into what neural signals the nervous system may receive due to the dynamic forces experienced as the animal moves through its environment.

Despite many insect-like robots having been built in the past few decades, few robots directly incorporate insect-like load sensing [9]. Some robots such as Octavio have applied animal-like walking control networks to drive walking through a combination of sensory feedback and central pattern generators [10]. Despite the success of this study, the robot had only rudimentary ground contact sensing via a toggle switch, meaning that the robot could not measure the dynamics of force over the course of the step. In contrast, other robots such as Hubodog2 [11] and Drosophibot [12] have implemented animal-like load sensing in the legs by mounting strain gauges to the leg segments. However, it can be difficult to tune the bias of the amplifiers to set a threshold to determine ground contact white ensuring the load signal does not saturate. We hypothesize that using our dynamic CS model as a filter for strain measurements in a robot will alleviate both of these issues. The model is very sensitive to changing loads, enhancing transitions between stance and swing, and its model adapts its output in response to a constant load, meaning that amplifier bias may be canceled out over time.

In this study, we investigate what dynamic load feedback the nervous system may experience while the leg makes contact with the ground, supports and propels the body, and then breaks contact with the ground. We hypothesize that the dynamics of the CS will accentuate increases in load at the initiation of stance while eliminating the others. We also hypothesize that these features are robust to changes in sensor configuration. For example, weight can be added to the leg and the servomotor's P gain can be changed without greatly affecting responses to increasing and decreasing load.

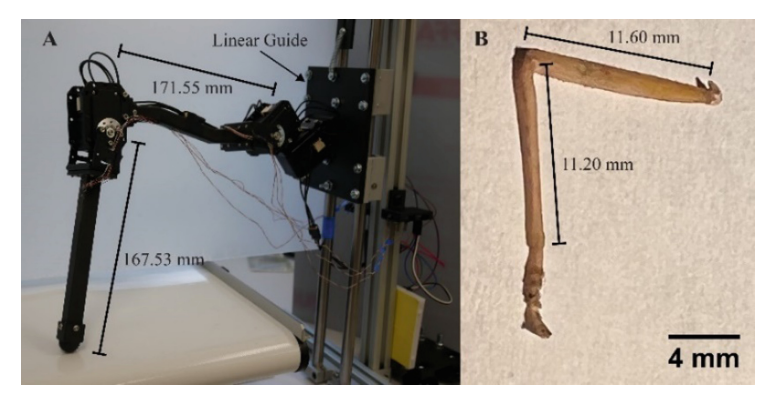


**Fig. 1.** A) Robotic model of the middle leg of *Carausius morosus* attached to linear guide. The linear guide can only move in the vertical direction (Z axis). As the leg steps on the treadmill, the linear guide is free to move, meaning that the leg must support its weight when stepping. B) A *Carausius morosus* middle leg for comparison to its biological counterpart.

## 2 Methods

#### 2.1 Robotic Leg Construction

The robotic leg in Fig. 1 consists of three MX-28 dynamixel servomotors along with 3D printed parts, which were used to construct a 14.79:1 scale model with the same segmental proportions as the middle leg of the stick insect *Carausius morosus* (*C. morosus*) [13, 14]. Figure 2 shows the leg with the thorax-coxa (ThC), coxa-trochanter (CTr), and femur-tibia (FTi) joint axes labeled. The proximal servomotor (ThC) is attached to a linear guide to simulate the weight and movement of the insect body. Two strain gauge rosettes on the leg capture the strain data and are connected to operational amplifiers to boost the signal. Each rosette measures the transversal and axial strain of the leg segment. The location and orientation of the rosettes is comparable to the location and orientation of major CS groups on the stick insect leg: the proximal femur rosette measures axial (CS group 3) and transversal (CS group 4) strain, and the proximal tibia rosette measures axial (CS group 6B) and transversal (CS group 6A) strain [2, 7]. An OpenCM 9.04 microcontroller converts the analog amplified strain signal into a 12-bit digital signal that is sent to the control computer over a serial connection.

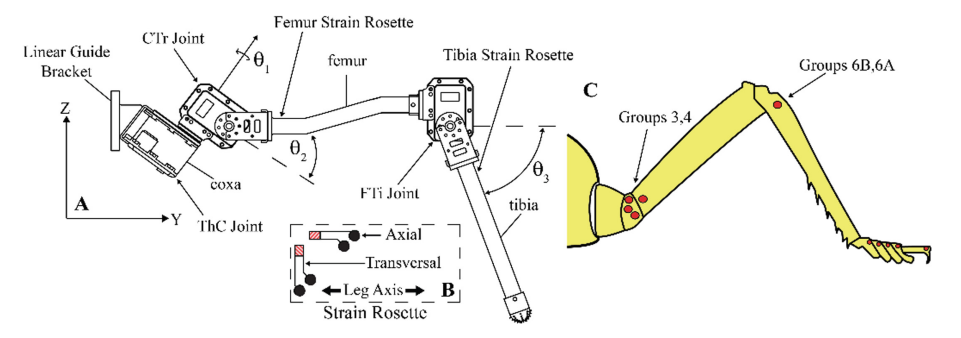


**Fig. 2.** A) 3 degree of freedom robotic model of the middle leg of *C. morosus*. Joint axes, joint angle measurements, and leg segments are labeled. The locations of strain rosettes are indicated. B) The inset shows the orientation of each strain rosette relative to the long axis of the leg segment on which it is mounted. C) An illustration of a *C. morosus* leg indicating locations of CS groups.

#### 2.2 Robot Forward and Inverse Kinematics

The kinematic model for the system has the same degrees of freedom as the insect [13, 14]. Great care was taken to properly scale the kinematics of the *C. morosus* middle leg for the robot (values in Table 1). The kinematic spatial (i.e., global coordinate system) chain was constructed with the product of exponentials,

$$g_d = e^{\hat{\xi}_1 \theta_1} e^{\hat{\xi}_2 \theta_2} e^{\hat{\xi}_3 \theta_3} g_{st} \tag{1}$$

where  $\theta_1$  is the angle of the ThC joint,  $\theta_2$  is the angle of the CTr joint, and  $\theta_3$  is the angle of the FTi joint [15]. The matrix exponentials produce the augmented  $4 \times 4$  matrix  $g_d$ ,

, which contains the rotation matrix and coordinates of the end effector (i.e., the foot) in relation to the spatial reference frame.  $g_{st}(0)$  describes the end effector in the leg's zero configuration, that is, when the leg is in its neutral posture. Each joint's impact on the end effector's position and orientation is described by the augmented matrix  $e^{\hat{\xi}_n\theta_n}$ .  $\hat{\xi}_n$  represents the axis of rotation for the  $n^{th}$  joint.

**Table 1.** Vectors of model parameters in zero configuration.  $\omega$  is a unit vector in direction of twist, q is point on the axis of rotation (mm)

Zero Configuration Vectors			
	X	у	Z
$\omega_1$	0	-sin (37°)	-cos (37°)
$\omega_2$	1	0	0
ω3	1	0	0
$q_1$	0	63.35	17.30
$q_2$	0	91.39	19.62
$q_3$	0	228.41	-83.62
<i>q</i> <sub>end</sub>	0	360.69	-183.28

The footpath was modeled and scaled after that of *C. morosus* [13]. To calculate the inverse kinematics, Newton-Raphson determined the necessary angles to achieve the footpath in Fig. 3. Because the leg has 3 non-parallel joint axes, there is a unique set of joint angles that places the foot in any particular 3D position in space.

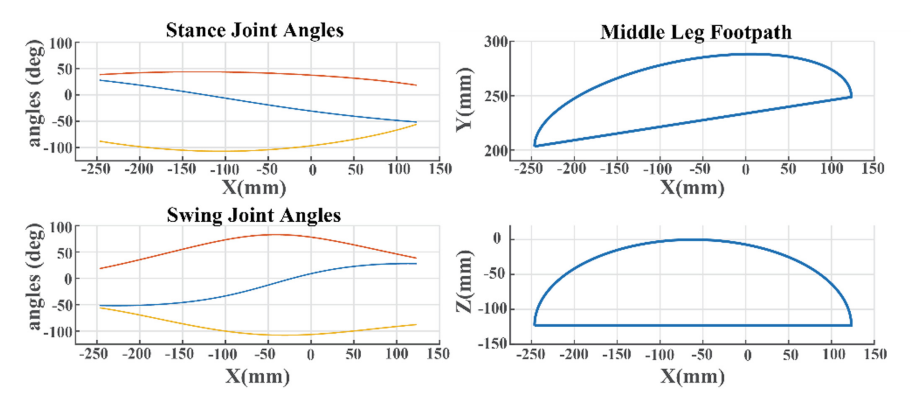


**Fig. 3.** Left graphs show stance and swing angles of robotic *C. morosus* middle leg (ThC upper, CTr middle, FTi lower) plotted against the x-coordinate of the foot in space as in [13]. The swing phase and stance phase each last 2 s. The right graphs show the projected scaled footpath of the *C. morosus*. The upper right graph is projected in the y-x plane, the lower right graph is projected in the z-x plane.

#### 2.3 Robotic Control

Data was collected using a MATLAB script to command servomotor angles through the OpenCM 9.04 microcontroller acting as an intermediary. On a desktop computer, the MATLAB script solved the inverse kinematics problem to calculate angle commands for the servomotors that would generate the desired foot path. The script sent the angle commands over a serial connection to the OpenCM 9.04 microcontroller. The OpenCM broadcasted the angle commands to the servomotors in the leg, and then returned the current servomotor angles and strain gauge readings, converted from analog to a 12-bit digital value, to the desktop computer.

## 2.4 Treadmill and Dynamic Scaling

The robotic leg stepped on a treadmill to simulate pushing the body forward. Because the ThC servomotor was mounted to a linear guide which is a vertically-sliding carriage, the leg also supported the carriage's weight during each stance phase. The treadmill's speed was matched to the stepping of the leg. The treadmill speed was synced with the use of a calibrated tachometer.

To ensure that the robot is dynamically scaled to the insect, that is, that it experiences a similar balance of inertial, viscous, elastic, and gravitational forces, the stepping cycle of the robot must be scaled to its dynamics in the same way as the animal's. In particular, the cycle period needs to be proportional to the natural frequency of the leg oscillation in both the animal and the robot. Insects are quite small, and gravity does not affect them considerably; similarly, when the robot is powered on, the leg is supported against gravity. This means that the leg does not act like a pendulum, but like a spring and mass. As a result, the natural frequency depends on the elastic stiffness of the joints and the moment of inertia of their limbs. A C. morosus leg is approximately a 11 mg [13] slender rod and the stiffness around the femur tibia joint is approximately  $10^{-6}$  Nm/rad [19]. This means the natural period is 0.132 s, so a step of one second is 6 times longer than the natural period. The robotic leg follows the same characteristic. Its main source of inertia is the moment of inertia of the servomotor rotor which is approximately  $1 \times 10^{-2} \,\mathrm{kgm^2}$ , and the stiffness is approximately 1 Nm/rad. This gives the robotic leg a natural period of 0.63 s, so four seconds is the dynamically scaled step time of the robotic leg, also 6 times longer than the natural period.

#### 3 Results

The robotic leg of the *C. morosus* completed 50 sequential steps in its baseline configuration (no weight added to the linear guide's carriage, default servomotor P gain) for Fig. 4. Data collected from each of the two strain gauge rosettes gave the axial and transversal strain of the femur and tibia. The geometry of the leg and orientation of the strain sensors gave a great deal of information about each other. The axial strain of the femur is the largest because this segment primarily supports the weight of the body, and it continues to increase after stance begins as it aligns the plane of the leg with gravity. As it rotates past the vertical orientation, the signal decreases. The transversal strain has

about 1/3 the amplitude and the opposite sign of the axial strain, consistent with the Poisson's ratio of typical solid materials.

The model output in Fig. 5 shows that the responds of the femur axial CS (Group 3) greatly increased at the onset of stance. Once stance was half completed and strain began do decrease, Group3's response was silenced. The same situation was seen with tibia axial CS (Group 6B) and tibia transversal CS (Group6A), albeit on a smaller scale as strain is smaller for the tibia [14]. Note the peak CS discharges at the beginning and end of stance phase.

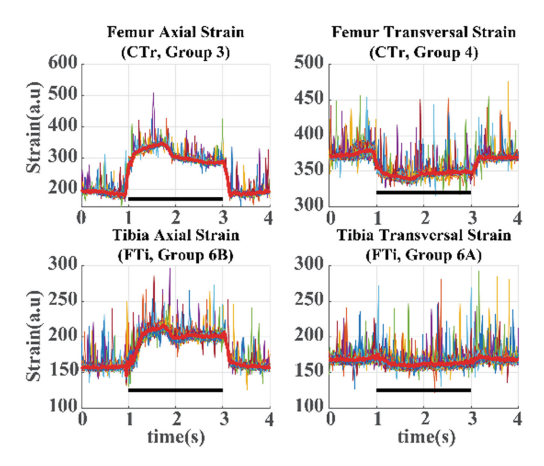


**Fig. 4.** Raw strain data from every strain gauge from 50 robot steps, with the average overlaid in red and stance phase represented by the black bar. Positive changes in values indicate compression; negative changes in values indicate tension. The Y axis has arbitrary units of strain (Color figure online).

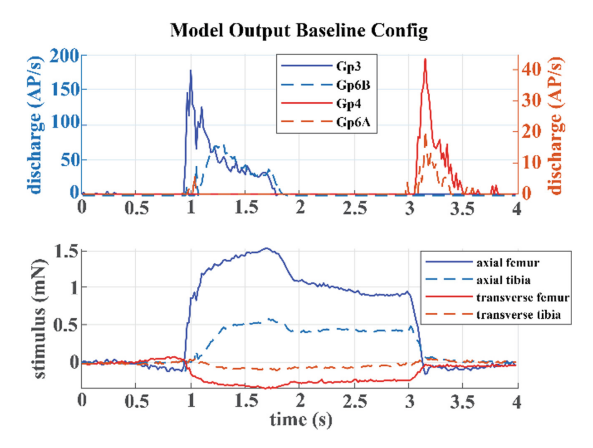
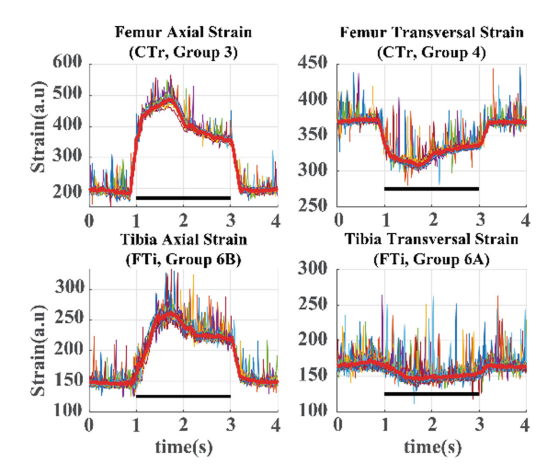


Fig. 5. Model CS output for mean of 50 steps in baseline configuration.

In Fig. 6, the leg walked 50 steps, with the linear guide weighed down with an extra 500 g. The shape of the strain for both the femur and tibia remained relatively unchanged

from Fig. 4, except the amplitude increased. The model CS data in Fig. 7 also reflects what was seen in Fig. 5, with strong signaling at the beginning and end of stance phase. Group 3 was activated on the onset of stance then deactivated halfway through stance once the leg plane flipped orientation. Group 4 increased once the leg was unloaded, signaling that the stance phase had ended. Group 6B shows a similar pattern, with Group 6A activating at the end of stance. It should also be noted that the model response had a better signal-to-noise ratio as the strain increased. This was particularly evident in Groups 6A and 6B because the strain was relatively small compared to Groups 3 and 4.



**Fig. 6.** Raw strain data of 50 steps with additional 500 g, with the average overlaid in red. Stance phase is represented by a black bar. Positive change in values indicate compression, negative change in values indicate tension. Y axis has arbitrary units of strain (Color figure online).

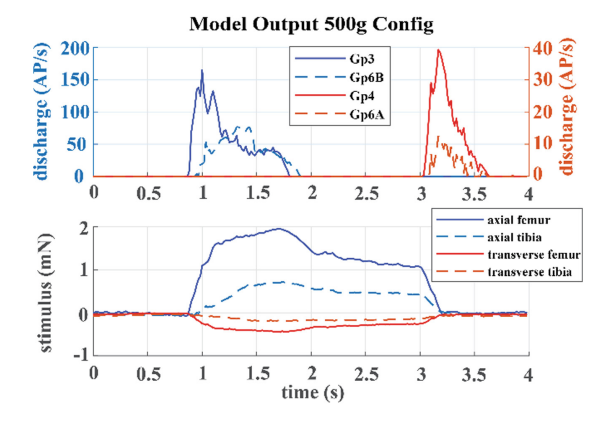
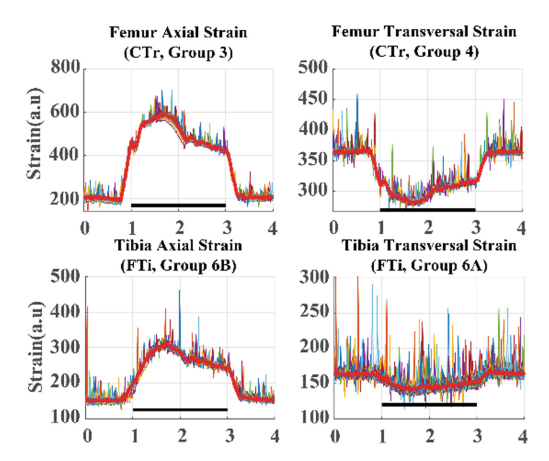


Fig. 7. Model CS output for a mean of 50 Steps with an additional 500 g (Color figure online).

Figure 8 includes an additional 50 leg steps but with 1000 g of extra weight. The amplitude of the strain on the tibia and femur increased further compared to previous

loading conditions. The shape of the strain response remained approximately unchanged despite the large increase in weight. While the model CS responses in Fig. 9 are generally similar to past trials, the exception is Group 3, whose responses show large fluctuations in discharge over time. This is because the "ripple" in the load signal is amplified under larger weight, and the CS model is sensitive to changing loads.



**Fig. 8.** Raw Strain data of 50 steps with additional 1000 g, with the overlay of average in red; stance phase is represented by a black bar; Positive change in values indicate compression, negative change in values indicate tension; Y axis has arbitrary units to signify strain (Color figure online).

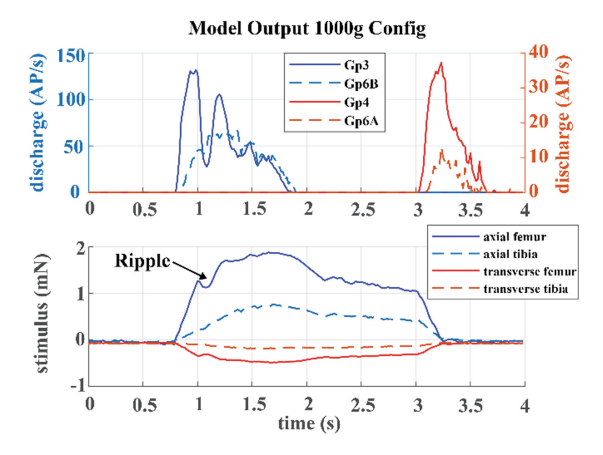
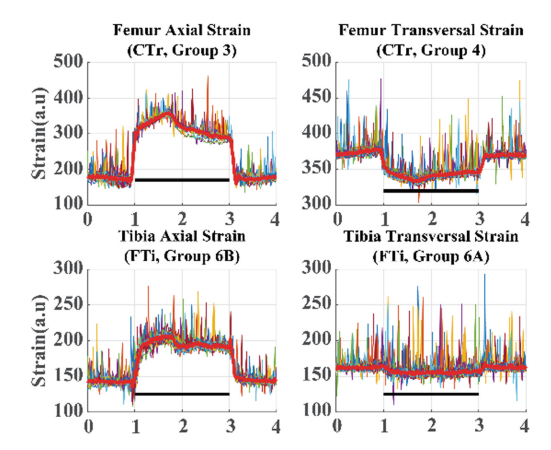


Fig. 9. Model output for mean of 50 Steps and an additional 1000 g

Data in Fig. 10 was collected after doubling the servomotor P gain, which approximately doubled the stiffness of the leg. No additional weight was added. Like the other configurations, Fig. 11 shows Group 3 activates at the start of stance and deactivates once the load decreases. Group 4 did the opposite. Group 6A and 6B followed suit, but at lower strain levels. It should also be noted that the increased stiffness helped reduce the bounce of the leg upon impact.



**Fig. 10.** Raw stain data with servomotor P gain doubled with the average overlaid in red. Stance phase is represented by a black bar. Positive change in values indicate compression; negative change in values indicate tension. The Y axis has arbitrary units of strain (Color figure online).

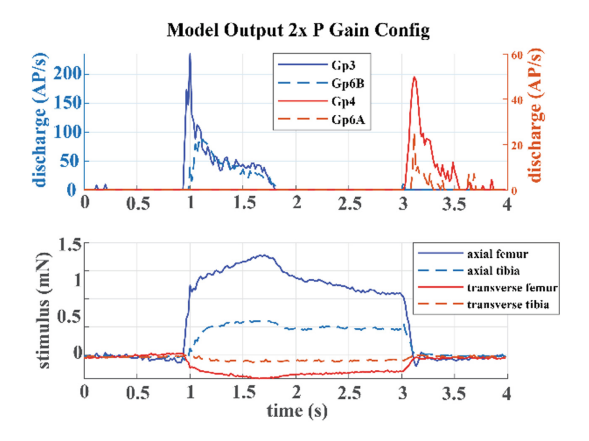


Fig. 11. Model output for a mean of 50 steps with doubled P gain

## 4 Discussion

In this study, strain data was collected simultaneously from four different locations on a dynamically scaled robotic model of a *C. morosus* middle leg. It is challenging to collect such data from the animal itself, and even successful attempts at recording from CS in behaving animals have been limited in scope [6, 7, 17]. With this robotic model, we can estimate the sensory signals that the nervous system may receive from all over the leg.

We applied a dynamic CS model [5] to filter the average strain data. This filter accentuates the dynamic changes in force that occur when stance phase begins and ends. These are critical events to the timing of stepping across the legs [18, 19]. Since the timing of load is so important to the coordination of the stepping of an insect's multiple legs [1, 4, 18, 19], a robot that employs such filtering may have improved coordination compared

to a robot that does not. We will explore this idea in future studies by implementing this dynamic CS model in a closed-loop walking controller for a six-legged robot. We hypothesize that dynamic load sensing will produce interleg coordination that is robust to changes in body weight or actuator properties.

Our study has several limitations. For example, in Fig. 5 the tibia transversal strain was quite small, resulting in a poor signal-to-noise ratio. However, this is unsurprising because the tibia is nearly aligned with gravity during walking, meaning that it experiences very little bending moment. Furthermore, due to the Poisson Effect, the transversal sensor only experiences about 1/3 the strain of the axial sensor [7]. Another complication was the bouncing of the leg at the start of stance phase for the baseline configuration. It seems unlikely that the animal would experience similar bouncing, because it actively grips the substrate. Changing the weight of the body or stiffness of the servomotors greatly reduced the bounce, suggesting that this bounce was due to resonance in the leg's mechanics. In the future, we plan to add an active tarsus with which to grip the substrate, which may reduce bounce. We also plan to further explore the effects of the leg's material properties on the sensory signals.

## 4.1 Comparison to Biomechanics and Neurophysiology

The linear guide was a critical part of the experiment because it allowed for the recording of the leg strain due to the leg's and linear guide's weight and not the strain of the leg pushing against a fixed bracket. As a result, the posture of the leg could change but the applied force was nearly constant, just as in walking. Preliminary experiments in stick insects suggest that CS respond differently between the controlled force, uncontrolled posture condition as we tested in this study and the constrained posture, uncontrolled force condition that is typical for experiments characterizing CS responses [5, 20–22]. Despite our robot only being one leg, we may be capturing important features of leg loading, that is, controlling the force but not constraining the posture.

The model could reliably distinguish the start and end of stance phase. This is evidenced by high-amplitude discharge from Groups 3 and 6B at the start of stance with relatively invariant amplitude and silencing when the force decreased. Groups 4 and 6A showed the opposite trend, with high-amplitude discharge at the start of swing and silencing by the end of swing. These results mimic the active signaling of unloading that has been described in insect CS [1, 6].

It is important to note that our model emulates the characteristics of the larger CS rather than the smaller, more tonic CS. In ramp and hold tests, tonic receptors show more prolonged discharges and incomplete adaptation to sustained loads [20, 21]. This could produce discharges throughout the stance phase, unlike Groups 3 and 6B in our robotic model. In addition, the discharges of receptors of opposite orientations (i.e., Group 3 vs. Group 4, Group 6B vs. 6A) are completely reciprocal in tests using ramp and hold force application and release in the leg plane. Similar reciprocal patterns of activity are seen both in the model simulations and in biological experiments in partially restrained animals showing "single leg stepping" [22].

The results of the robotic leg and model suggest new experiments in the biological system that could test this interpretation. Although technically challenging, it would be beneficial to examine the responses of the tibial sensilla to forces applied to the leg

using the waveforms of strain seen in the present study, including those obtained when additional loads must be supported.

## 4.2 Application to Robotics

The type of dynamic sensing presented in this study may improve the practicality of strain gauges in legged robots by making it easier to calibrate the sensors. This is important because simplifying calibration may reduce the burden of designing robots with many redundant sensors as seen in animals [9, 13]. We hypothesize that robots would be more graceful if they utilized more sensory feedback from additional modalities, as animals do [13, 23]. More robust sensory filtering may eliminate the need for careful calibration, removing one engineering hurdle to building robots with orders of magnitude more sensors.

**Acknowledgments.** This work was supported by NSF IIS 2113028 as part of the Collaborative Research in Computational Neuroscience Program. A special thanks to Clarissa Goldsmith for providing the necessary experimental data on the MX-28 dynamixel servomotors.

#### References

- Zill, S.N., Schmitz, J., Büschges, A.: Load sensing and control of posture and locomotion. Arthropod Struct. Dev. 33, 273–286 (2004). https://doi.org/10.1016/j.asd.2004.05.005
- Delcomyn, F., Nelson, M.E., Cocatre-Zilgien, J.H.: Sense organs of insect legs and the selection of sensors for agile walking robots. Int. J. Rob. Res. 15, 113–127 (1996). https://doi.org/10.1177/027836499601500201
- Mohren, T.L., Daniel, T.L., Eberle, A.L., Reinhall, P.G., Fox, J.L.: Coriolis and centrifugal forces drive haltere deformations and influence spike timing. J. R. Soc. Interface 16(153), 20190035 (2019). https://doi.org/10.1098/rsif.2019.0035
- Duysens, J., Clarac, F., Cruse, H.: Load-regulating mechanisms in gait and posture: comparative aspects. Physiol. Rev. 80, 83–133 (2000)
- Zill, S.N., Dallmann, C.J., Szczecinski, N., Büschges, A., Schmitz, J.: Evaluation of force feedback in walking using joint torques as "naturalistic" stimuli. J. Neurophysiol. 126, 227– 248 (2021). https://doi.org/10.1152/jn.00120.2021
- Keller, B.R., Duke, E.R., Amer, A.S., Zill, S.N.: Tuning posture to body load: Decreases in load produce discrete sensory signals in the legs of freely standing cockroaches. J. Comp. Physiol. A. 193(8), 881–891 (2007). https://doi.org/10.1007/s00359-007-0241-y
- Ridgel, A., Frazier, F., Zill, S.: Dynamic responses of tibial campaniform sensilla studied by substrate displacement in freely moving cockroaches. J. Comp. Physiol. A 187(5), 405–420 (2001). https://doi.org/10.1007/s003590100213
- Szczecinski, N.S., Dallmann, C.J., Quinn, R.D., Zill, S.N.: A computational model of insect campaniform sensilla predicts encoding of forces during walking. Bioinspir. Biomim. 16, 065001 (2021). https://doi.org/10.1088/1748-3190/ac1ced
- 9. Manoonpong, P., et al.: Insect-inspired robots: bridging biological and artificial systems. Sensors 21(22), 7609 (2021). https://doi.org/10.3390/s21227609
- von Twickel, A., Hild, M., Siedel, T., Patel, V., Pasemann, F.: Neural control of a modular multi-legged walking machine: Simulation and hardware. Robot. Auton. Syst. 60(2), 227–241 (2012). https://doi.org/10.1016/j.robot.2011.10.006

- Sim, O., Jung, T., Lee, K.K., Oh, J., Oh, J.-H.: Position/torque hybrid control of a rigid, high-gear ratio quadruped robot. Adv. Robot. 32(18), 969–983 (2018). https://doi.org/10.1080/01691864.2018.1516162
- Goldsmith, C.A., Szczecinski, N.S., Quinn, R.D.: Neurodynamic modeling of the fruit fly Drosophila melanogaster. Bioinspir. Biomim. 15(6), 065003 (2020). https://doi.org/10.1088/ 1748-3190/ab9e52
- Cruse, H., Bartling, C.: Movement of joint angles in the legs of a walking insect, *Carausius morosus*. J. Insect Physiol. 41, 761–771 (1995). https://doi.org/10.1016/0022-1910(95)000 32-P
- Theunissen, L.M., Bekemeier, H.H., Dürr, V.: Comparative whole-body kinematics of closely related insect species with different body morphology. J. Exp. Biol. 218, 340–352 (2015). https://doi.org/10.1242/jeb.114173
- Lynch, K.M., Park, F.C.: Modern Robotics: Mechanics, Planning, and Control, 1st edn. Cambridge University Press, USA (2017)
- Hooper, S.L., et al.: Neural control of unloaded leg posture and of leg swing in stick insect, cockroach, and mouse differs from that in larger animals. J. Neurosci. 29(13), 4109–4119 (2009). https://doi.org/10.1523/JNEUROSCI.5510-08.2009
- Noah, J.A., Quimby, L., Frazier, S.F., Zill, S.N.: Sensing the effect of body load in legs: Responses of tibial campaniform sensilla to forces applied to the thorax in freely standing cockroaches. J. Comp. Physiol. A 190(3), 201–215 (2004). https://doi.org/10.1007/s00359-003-0487-y
- 18. Cruse, H.: What mechanisms coordinate leg movement in walking arthropods? Trends Neurosci. 13, 15–21 (1990). https://doi.org/10.1016/0166-2236(90)90057-H
- Dallmann, C.J., Hoinville, T., Du, V., Schmitz, J.: A load-based mechanism for inter-leg coordination in insects. 284 (2017). https://doi.org/10.1098/rspb.2017.1755
- Zill, S., Büschges, A., Schmitz, J.: Encoding of force increases and decreases by tibial campaniform sensilla in the stick insect, *Carausius morosus*. J. Comp. Physiol. A 197, 851–867 (2011)
- 21. Zill, S., Schmitz, J., Chaudhry, S., Büschges, A.: Force encoding in stick insect legs delineates a reference frame for motor control. J. Neurophysiol. **108**, 1453–1472 (2012)
- Zill, S., Chaudhry, S., Büschges, A., Schmitz, J.: Directional specificity and encoding of muscle forces and loads by stick insect tibial campaniform sensilla, including receptors with round cuticular caps. Arthr. Struct. Dev. 42, 455–467 (2013)
- Dallmann, C.J., Karashchuk, P., Brunton, B.W., Tuthill, J.C.: A leg to stand on: computational models of proprioception. Curr. Opin. Physiol. 22, 100426 (2021). https://doi.org/10.1016/j. cophys.2021.03.001